Assimilation of MSG land-surface temperature into land-surface model simulations to constrain estimates of surface energy budget in West Africa

P. P. Harris, C. M. Taylor, Centre for Ecology and Hydrology, Wallingford, U.K.

Email: ppha@ceh.ac.uk

1. Introduction

In the semi-arid regions of West Africa the surface energy partition is related closely to near surface moisture availability. Such moisture availability exhibits marked heterogeneity at scales of a few kilometres, related to the passage of storm systems during the previous one or two days. The associated variations in surface fluxes affect planetary boundary layer properties at the mesoscale, which may in turn affect rainfall and the seasonal development of the West African monsoon.

Atmosphere models used to study this land-atmosphere coupling are sensitive to the soil moisture initial condition. There exists no observation network for soil moisture in West Africa, so models rely on data from atmosphere analyses, which are often unable to describe adequately surface variation at the mesoscale. Additionally, retrospective estimates of the seasonal surface energy and water budgets using land-surface models are biased by persistent model errors in soil moisture. Anomalies in near-surface (top few centimetres) soil moisture are anti-correlated with anomalies in land-surface brightness temperature, which is observed by the SEVIRI thermal infra-red sensors onboard the Meteosat Second Generation (MSG) satellites. Here, we present methods developed for assimilating the MSG land-surface temperature product from the Land SAF to constrain estimates of the surface energy and water budgets using the JULES land-surface model. This MSG temperature product has a pixel size of approximately 3 km in this region, and is known to provide information of surface wetness anomalies at the scales of interest. The results will provide, for a large region of West Africa, improved initial conditions for modelling studies and seasonal estimates of the surface energy and water budgets.

2. Data

The land surface temperature (LST) observations used were the Land SAF[1] LST product derived from thermal radiances measured by the SEVIRI instrument on-board the Meteosat Second Generation platforms (Sobrina and Romaguera, 2004). These LST observations have a typical spatial resolution of 3 km in the Sahel and images are produced continually every 15 minutes. A recent study of the atmospheric boundary layer during the AMMA campaign (Taylor et al, 2007) confirmed that features in these LST data that persist over a few days are associated with spatial variation in boundary layer temperature, humidity and wind.

For this study, additional screening of these LST data based on temporal evolution of thermal and visible SEVIRI channel radiances was applied to reject cloud- and dust-contaminated pixels. Assimilated data are restricted to the period of 22nd June 2006 to 10th October 2006 for daylight hours of 0630 UTC to 1700 UTC.

The JULES[2] land surface model was forced with near-surface climate data prepared for ALMIP[3] for the years 2001 to 2006 inclusive, which include rainfall estimates produced by AMMA-SAT. These forcing data have a pixel resolution of 0.5° (approx. 50 km), much coarser than the available LST observations. The ALMIP pixel size, however, does not resolve adequately surface moisture and heat flux features of interest, which are typically 10s of km, so JULES was run for each SEVIRI pixel under the same ALMIP forcing. Herein, initial results are presented for a single ALMIP pixel centered at (1.5°E, 15.5°N).

3. Method

Here a variational method is used to diagnose increments at the SEVIRI-scale to the ALMIP-scale rainfall forcing that gives the best simulation of the observed LST by JULES over a finite time window. A variational rather than a sequential method was chosen because (i) LST observations are available at a similar frequency as model state LST, and (ii) the final analysed model state remains a true model trajectory. The cost function minimised is,

$$
\begin{aligned}
J(\delta \boldsymbol{P}) &= J(\delta \boldsymbol{P})_b \quad + \quad J(\delta \boldsymbol{P})_{obs} \\
&= \delta \boldsymbol{P}^T \boldsymbol{B}^{-1} \delta \boldsymbol{P} \quad + \quad (\boldsymbol{T}_{obs} - \boldsymbol{h}(\delta \boldsymbol{P}))^T \boldsymbol{R}^{-1} (\boldsymbol{T}_{obs} - \boldsymbol{h}(\delta \boldsymbol{P}))
\end{aligned}
$$

Where $\delta \boldsymbol{P}$ is a vector of rainfall increments for model time steps with non-zero rainfall in the one-day window; $\boldsymbol{T}_{obs}$ is a vector of LST observations that are available in the three-day window; $\boldsymbol{h}(\delta \boldsymbol{P})$ is JULES simulated LST through the three-day window; $\boldsymbol{B}$ is the error covariance matrix for rainfall increments; $\boldsymbol{R}$ is the observation error covariance matrix. The 'background' term provides a constraint based on uncertainty in the forcing rainfall, and the 'observation' term provides a constraint based on model/observed LST differences (innovations) and uncertainty in the LST observation. At present, the method does not account for biases in the model or observations.

Figure 1 shows how Rainfall increments for day one are diagnosed by minimising the cost function using innovations though days one to three. The windows are then shifted forward by one day and the process repeated to diagnose rainfall increments for day two based in innovations for days two to four, and so on. Rainfall increments are diagnosed only at times when there is non-zero rainfall in the forcing dataset, and increment amounts are constrained to lie in the range (-*P*, 10 mm day^{-1}) at each model time step.

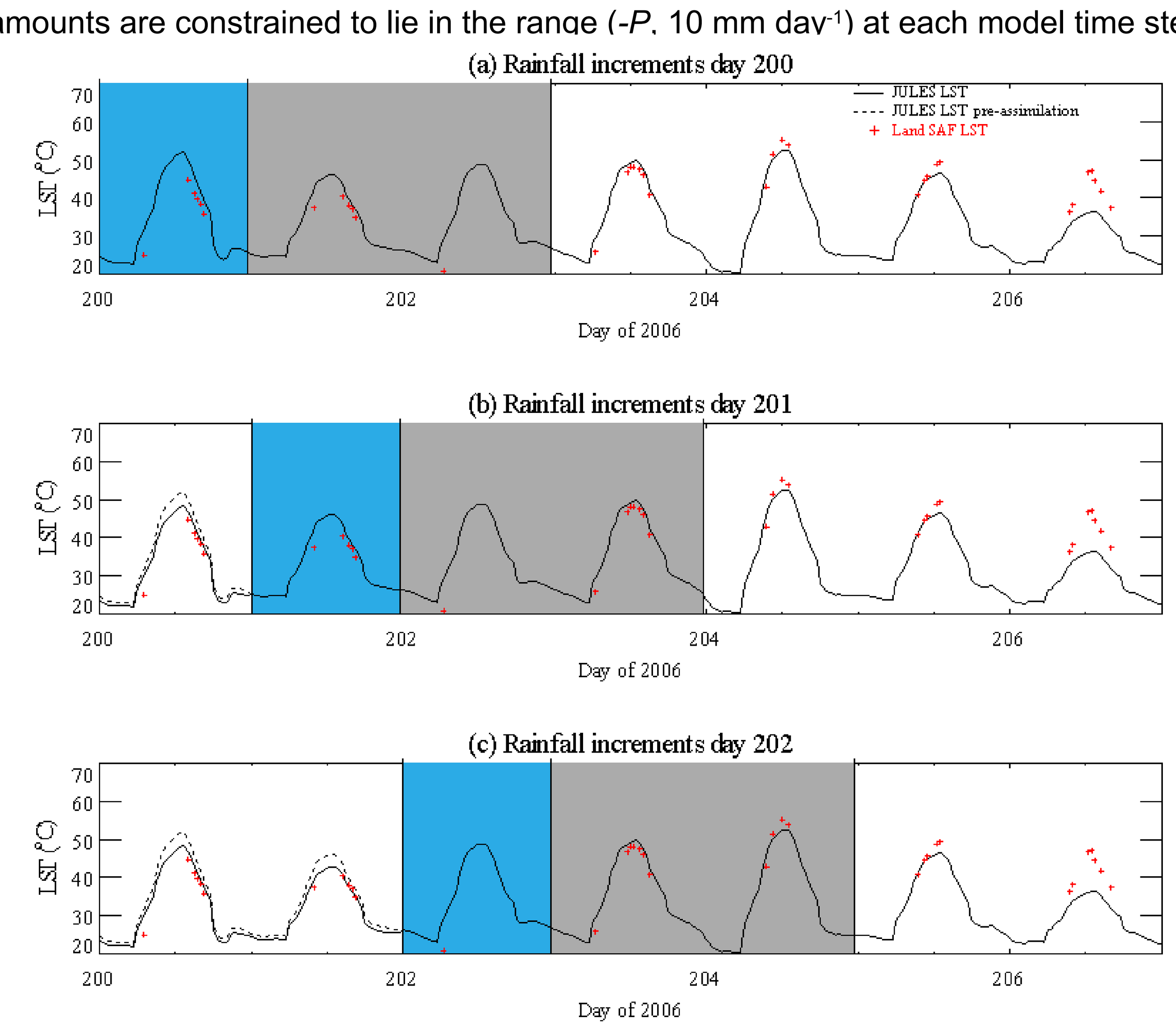

Fig 1. Schematic showing how the assimilation scheme uses model minus observed LST innovations over a 3-day window (blue plus grey shading) to analyse rainfall increments over a 1-day window (blue shading only). Model LST prior to assimilation is shown as dashed line.

4. Results

Assimilation of Land SAF LST reduces ALMIP-pixel mean bias LST from +3.0 K to +1.9 K and RMSE from 6.4 K to 4.7 K. The pixel mean total rainfall increment for 2006 was +53 mm, or 29% of the forcing rainfall total, with a range across SEVIRI-pixels of -30 mm to +90 mm. This tendency for the scheme to add water to the model is indicative of bias in the innovations due primarily to model bias. The effect of this bias will be addressed in future versions of the assimilation method.

Figure 2 shows surface soil moisture as a percentage of saturation for 31st July 2006 for the single ALMIP pixel. The model state shows distinct spatial heterogeneity in surface moisture within the domain, which has been added by the assimilation scheme. The map shows diagonally orientated surface moist patches characteristic of the north-east to south-west passage of mesoscale systems in the region.

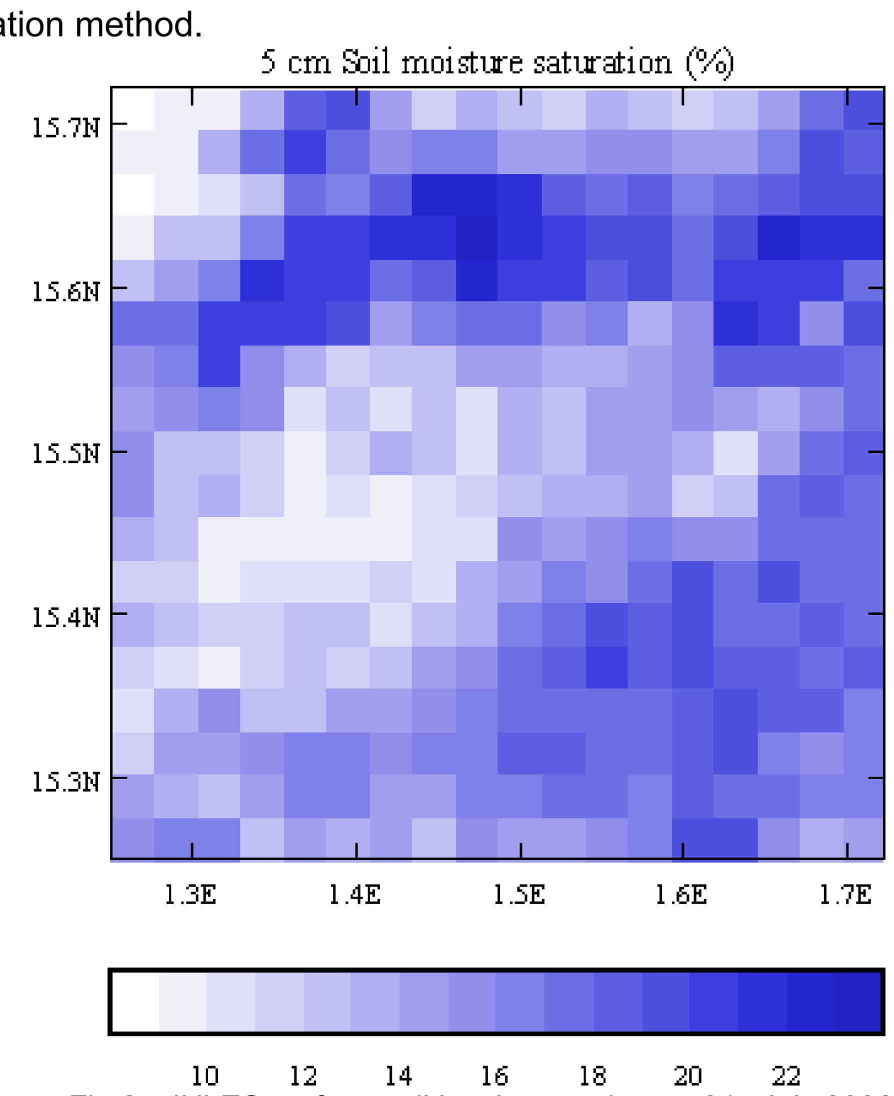

Fig 2. JULES surface soil level saturation on 31st July 2006 for a single 0.5° ALMIP pixel.

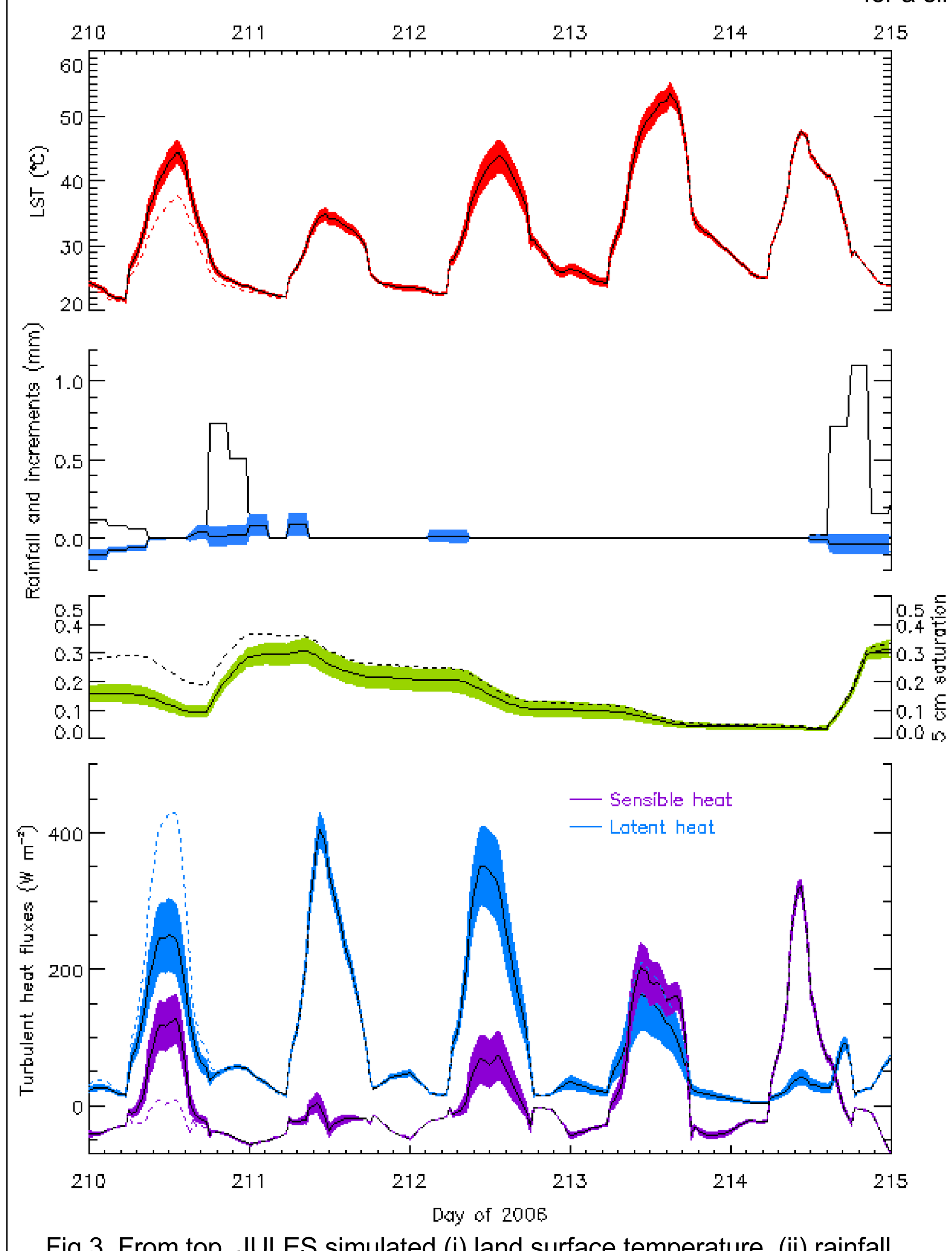

Fig 3. From top, JULES simulated (i) land surface temperature, (ii) rainfall and rainfall increments, (iii) soil surface saturation, (iv) sensible and latent heat flux for a single ALMIP pixel. Full lines and coloured bands indicate mean and standard deviation over all SEVIRI sub-pixels. Dashed lines indicate ALMIP pixel grid-box means prior to assimilation.

Figure 3 shows a typical time series of JULES surface state and fluxes through the period 29th July 2006 to 2nd Aug 2006 (days 210 through 215). On day 210, and on the preceding few days, the scheme reduced rainfall across the domain to increase the surface temperature, which reduced surface moisture and yielded a significant change to the ALMIP-pixel mean surface energy partition through day 210.

A rainfall event overnight on day 210 produced strong evaporation on day 211 with little sub-pixel variation. Over the next few days, however, spatial variation in surface moisture (Fig. 2) produced variation in surface energy fluxes across the domain. These fluxes are qualitatively consistent with the boundary layer properties observed by Taylor et al (2007) along a transect through this domain.

These results demonstrate how satellite LST observations may be combined usefully with land surface model simulations to provide finer-scale estimates of the surface state and fluxes in regions where the surface energy partition is governed strongly by surface moisture availability. The method will be developed further to include a better description of errors in rainfall forcing and to account for model bias.

References

[1] LandSAF – EUMETSAT Land Satellite Application Facility – http://landsaf.meteo.pt/

[2] JULES – Joint UK Land Environment Simulator – http://www.jchmr.org/jules/index.html

[3] ALMIP – AMMA Land surface Model Intercomparison Project – http://www.cnrm.meteo.fr/amma-moana/amma_surf/almip/index.html

Sobrina J.A. and Romaguera M. (2004) *Land surface temperature retrieval from MSG1-SEVIRI data*, Rem. Sens. Environ., 92 (2): 247-254.

Taylor C.M., Parker D.J. and Harris P.P. (2007) *An observational study of mesoscale atmospheric circulations induced by soil moisture*, Geophys. Res. Letts., 34, L15801, doi:10.1029/2007GL030572